SCIENCE CHINA
Technological Sciences

June 2010 Vol.53 No.6: 1612–1619
doi: 10.1007/s11431-010-3113-6

Blank design optimization for stepped-section profile ring rolling

QIAN DongSheng & HUA Lin*

School of Materials Science and Engineering, Wuhan University of Technology, Wuhan 430070, China

Received August 8, 2009; accepted December 23, 2009

A stepped-section ring consists of two rectangular section rings, a big ring and a small ring, joined together. This kind of ring is difficult to process by the ring rolling technique because of its complex cross-sectional shape. Thus a reasonable blank design is necessary. In this paper, four blank designs, one is a rectangular cross-section and the other three are stepped-sections with different step volumes, are proposed and compared with each other using theoretical analysis, FE simulation and experiments. It is shown that three of the designs can lead to volume flow from small ring into big ring during rolling, which is disadvantageous for shape formation and dimensional precision; however, the other design may result in good ring shape and high dimensional precision. Therefore, the optimal blank design is determined to be the one in which the volumes of the big and small rings of the initial blank are equal to those of the final rings, respectively.

ring rolling, stepped-section ring, optimization design, FE simulation

Citation: Qian D S, Hua L. Blank design optimization for stepped-section profile ring rolling. Sci China Tech Sci, 2010, 53: 1612–1619, doi: 10.1007/s11431-010-3113-6

Nomenclature

R_0	Outer radius of rectangular section blank
r_0	Inner radius of blank
H_0	Thickness of rectangular section blank
B_0	Height of blank
R_{b0}	Outer radius of big ring of stepped-section blank
R_{s0}	Outer radius of small ring of stepped-section blank
H_{b0}	Thickness of big ring of stepped-section blank
H_{s0}	Thickness of small ring of stepped-section blank
B_{b0}	Height of big ring of stepped-section blank
B_{s0}	Height of small ring of stepped-section blank
L_0	Thickness of step of blank
R_b	Outer radius of big ring of rolled ring
R_s	Outer radius of small ring of rolled ring
r	Inside radius of rolled ring
H_b	Thickness of big ring of rolled ring
H_s	Thickness of small ring of rolled ring
B_b	Height of big ring of rolled ring
B_s	Height of small ring of rolled ring
L	Thickness of step of rolled ring
V_{b0}	Volume of big ring of blank
V_{s0}	Volume of small ring of blank
V_b	Volume of big ring of rolled ring
V_s	Volume of small ring of rolled ring

1 Introduction

Ring rolling is used to manufacture a wide range of mechanical parts, ranging from small bearings to large parts used in power generation plants, aircraft engines and cylindrical vessels [1]. Ring rolling has many advantages, such as high productivity, uniform quantity, smooth surface and material saving. It has been used in many industry fields, including aeronautics, astronautics, automobile, atomic energy, etc.

At present, much research on ring rolling has been carried out by experimental method [2, 3], analytical method [4–6] and finite element method [7–9], which study various

*Corresponding author (email: bestcx@yahoo.com.cn)

aspects like technology design [10, 11], deformation condition [12, 13] and material properties [14]. However, most of the research focused on rectangular section ring rolling and profile ring rolling was rarely investigated. For instance, ref. [15] estimated the pressure distribution, roll force and torque in T-section profile ring rolling based on the slip line method. Refs. [5] and [8] simulated the process of T-section profile ring rolling using the rigid-plastic FE method and elastic-plastic FE method, respectively. Ref. [16] studied the influences of rolling parameters on T-section profile ring rolling using the 3-D elastic-plastic FE method. Nevertheless, these studies all focused on T-section profile ring rolling. As seen in Figure 1, a stepped-section ring can be considered to consist of two rectangular section rings, that is, a big ring and a small ring, joined together. This kind of ring is difficult to process by the ring rolling technique because of its complex cross-sectional shape. At present, with no theoretical instruction, the technical design of stepped-section profile ring rolling is carried out through repeated rolling experiments, which consume a large amount of materials and time. So, stepped-section rings are now conventionally processed by machining, which has low productivity and large consumption.

Because different blanks can lead to different rolling results, blank design has important influence on the ring rolling process and is the first step of the technical design of ring rolling. The purpose of this paper is threefold: to investigate the blank design of stepped-section profile ring rolling, to put forward a valid blank design method, and to provide a theory basis for the technical design.

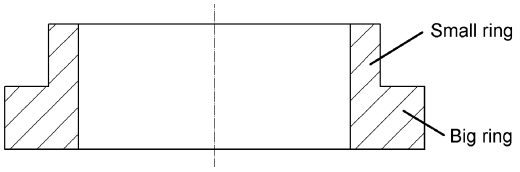

Figure 1 Stepped-section ring.

2 Methods

2.1 Four contact patterns between blank and roll gap

The cross-sectional shape of the blank should be the same as that of the rolled ring for easy forming and material saving. However, it is easier to process a rectangular section blank than a stepped-section blank. So, both the rectangular section blank and the stepped-section blank are considered in this paper, as shown in Figure 2.

The contact pattern between the blank and the roll gap depends on the shapes and dimensions of the blank and rolls, which directly influence the deformation condition of the blank in the rolling process. The shape and dimensions of the roll gap should match those of the rolled ring to obtain a rolled ring with specified dimensions.

Figure 3 shows the roll gap of stepped-section profile ring rolling. A closed roll gap limits the axial spread of the ring. The main roll has two working surfaces which contact with the exterior surfaces of the big and small rings, respectively. The mandrel has one working surface which contacts with the internal surface of the ring. R_1 is the outer radius of the main roll, R_{1b} and R_{1s} are the radii of the large and small working surfaces of the main roll. R_2 and R_{2w} are the outer radius and working radius of the mandrel. The two working surfaces of the main roll constitute a step, which is used to form the step of the rolled ring. So, the radial length of this

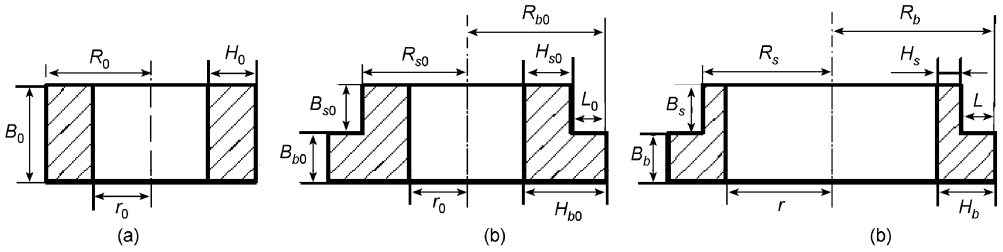

Figure 2 Blanks and rolled ring of stepped-section profile ring rolling. (a) rectangular section blank; (b) stepped-section blank; (c) stepped-section rolled ring.

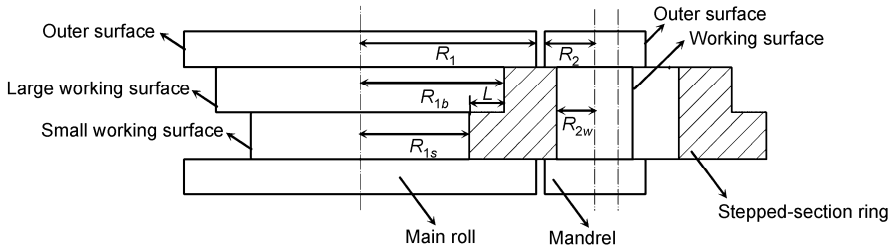

Figure 3 Roll gap of stepped-section profile ring rolling.

step is equal to the thickness of the step of the rolled ring, i.e.,

$$R_{1b} - R_{1s} = H_b - H_s = L . \quad (1)$$

When the dimension of the rolled ring is determined, the shape and dimension of the roll gap can be determined, too. By analysis, four contact patterns can be determined to exist in stepped-section profile ring rolling under different blank designs.

1) A rectangular section blank, in which the exterior surface of the blank only contacts with the large working surface of the main roll and the internal surface of the blank contacts with the working surface of the mandrel (Figure 4(a)).

2) A stepped-section blank with $L_0<L$, in which the exterior surface of the small ring contacts with the large working surface of the main roll, while the exterior surface of the big ring is suspended. The internal surface of the blank contacts with the working surface of the mandrel (Figure 4(b)).

3) A stepped-section blank with $L_0=L$, in which the exterior surfaces of the big and small rings contact with the small and the large working surfaces of the main roll, respectively. The internal surface of the blank contacts with the working surface of the mandrel (Figure 4(c)).

4) A stepped-section blank with $L_0>L$, in which the exterior surface of the big ring contacts with the small working surface of the main roll, while the exterior surface of the small ring is suspended. The internal surface of the blank contacts with the working surface of the mandrel (Figure 4(d)).

2.2 Four blank designs corresponding to the four contact patterns

The ratio of inside radius of the blank to that of the rolled ring is called the rolling ratio, K, which is defined as

$$K = \frac{r}{r_0} . \quad (2)$$

The value of K is selected according to the capability of the ring rolling mill [17]. When the value of K is determined, four blank designs corresponding to the above-mentioned four contact patterns can be proposed based on the volume conservation law in metal plastic deformation.

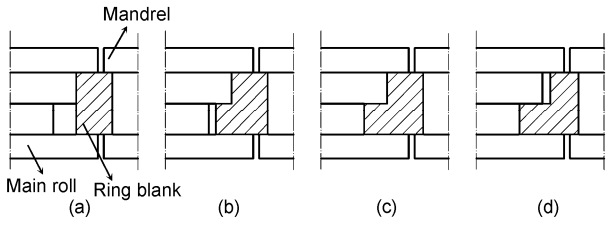

Figure 4 Four contact patterns of stepped-section profile ring rolling.

The dimensions of the rectangular blank (A1) satisfy

$$\pi(R_0^2 - r_0^2)B_0 = \pi(R_b^2 - r^2)B_b + \pi(R_s^2 - r^2)B_s . \quad (3)$$

The axial spread of the ring is very small because of the limitation of the closed roll gap. So, it is assumed that

$$B_0 = B , \quad B_{b0}=B_b , \quad B_{s0}=B_s . \quad (4)$$

According to eqs. (2), (3) and (4), the blank dimensions are designed as follows:

$$B_0=B , \quad r_0 = \frac{r}{K} , \quad R_0 = \sqrt{\frac{V}{\pi B} + r_0^2} , \quad (5)$$

where $V = \pi(R_b^2 - r^2)B_b + \pi(R_s^2 - r^2)B_s$ means the volume of the rolled ring.

According to eq. (4), the dimensions for stepped-section blank $L_0<L$ (A2) are designed and expressed as

$$B_{b0}=B_b , \quad B_{s0}=B_s , \quad r_0 = \frac{r}{K} ,$$
$$R_{b0} = \left(\sqrt{VB/\pi + B^2 r_0^2 - B_s B_b L_0^2} + B_s L_0\right)\Big/B , \quad (6)$$
$$R_{s0} = \left(\sqrt{VB/\pi + B^2 r_0^2 - B_s B_b L_0^2} - B_b L_0\right)\Big/B .$$

Using the same calculation, the dimensions of stepped-section blanks $L_0=L$ (A3) and $L_0>L$ (A4) are also expressed by eq. (6).

3 Analysis and discussion

3.1 Theoretical analysis

The volume conservation law in metal plastic deformation indicates that the blank volume is constant in rolling, but it does not mean that the volumes of the big and small rings are both constant in rolling. If there is volume flow between the big and small rings, it will interfere with the metal flow of the blank, and influence the dimensional accuracy of the rolled ring. To obtain a rolled ring with specified dimensions, the blank dimensions must compensate for any volume flow, which obviously increases the difficulty of blank design. So, it is significant to study the volume flow between the big ring and the small ring in rolling.

The apagoge method is used to study the volume flow between the big and small rings under the above-mentioned four design methods. By assuming that the volumes of the big and small rings are both constant in rolling, the dimensions of the rolled blank can be obtained based on the volume conservation law, and the assumption can be verified by comparing the dimensions between the rolled blank and the specified rolled ring. Using this method, the volume flow between the big and small rings is studied as follows.

(A1) The rectangular section blank

As seen in Figure 5, a rectangular section blank can also be divided into a big ring and a small ring. Because the outer radius of Part 1 will be larger than that of Part 2 after rolling, Part 1 and Part 2 are called the big ring and the small ring, respectively. According to geometrical relationships,

$$R_{b0}=R_{s0}=R_0,\ \ r_{b0}=r_{s0}=r_0,\ \ B_{b0}=B_b,\ \ B_{s0}=B_s, \tag{7}$$

with

$$\begin{aligned}\pi(R_b^2-r_b^2)B_b&=\pi(R_{b0}^2-r_0^2)B_{b0},\\ \pi(R_s^2-r_s^2)B_s&=\pi(R_{s0}^2-r_0^2)B_{s0},\end{aligned} \tag{8}$$

where r_b and r_s are the inside radii of the big and small rings of the rolled ring, respectively.

According to eqs. (7) and (8),

$$r_b^2-r_s^2=R_b^2-R_s^2. \tag{9}$$

It is obvious that $R_b>R_s$. Then, $r_b>r_s$, which means that the internal surface of the rolled blank is not a column surface. However, the internal surface of the actual rolled ring is a column surface, i.e., $r_b=r_s$. So, it can be determined that the assumption is invalid, and there is volume flow between the big and small rings in rolling.

Assuming that the blank can be formed as the specified rolled ring, one has

$$V_{b0}=\pi(R_{b0}^2-r_0^2)B_{b0},\ \ V_b=\pi(R_b^2-r^2)B_b. \tag{10}$$

Taking $\Delta V_b=V_b-V_{b0}$ as the volume change amount of the big ring of the blank, and combining eqs. (3) and (10), one can obtain the expression for ΔV_b:

$$\Delta V_b=\frac{\pi B_bB_s(R_b^2-R_s^2)}{B}. \tag{11}$$

It is obvious that $R_b>R_s$. Then, $\Delta V_b>0$. It is determined that the volume of the big ring increases, and the volume of the small ring can flow into the big ring in rolling under this design.

(A2) The stepped-section blank is designed with $L_0<L$. Using a similar derivation, one has

$$\begin{aligned}r_b^2-r_s^2&=(R_b+R_s)L-(R_{b0}+R_{s0})L_0,\\ \Delta V_b&=\frac{\pi B_bB_s(2R_bL-2R_{b0}L_0-L^2+L_0^2)}{B},\end{aligned} \tag{12}$$

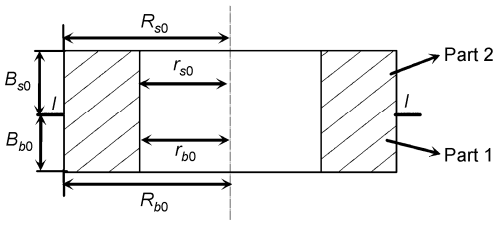

Figure 5 Rectangular section blank.

Because $R_b>R_{b0}$, $R_s>R_{s0}$ and $r>L>L_0$, $r_b>r_s$ and $\Delta V_b>0$. It is determined that the volume of the small ring can flow into the big ring in rolling under this design.

(A3) The stepped-section blank is designed with $L_0=L$. Using a similar derivation, one has

$$\begin{aligned}r_b^2-r_s^2&=(R_b+R_s)L-(R_{b0}+R_{s0})L_0,\\ \Delta V_b&=\frac{2\pi B_bB_sL(r_b-r_{b0})}{B}.\end{aligned} \tag{13}$$

Because $R_b>R_{b0}$, $R_s>R_{s0}$ and $r_b>r_{b0}$, $r_b>r_s$ and $\Delta V_b>0$. It is determined that the volume of the small ring can also flow into the big ring in rolling under this design.

(A4) The stepped-section blank is designed with $L_0>L$. Because $L_0>L$, it can be seen that the condition for $r_b=r_s$ exists, which is expressed as

$$\frac{L_0}{L}=\frac{R_b+R_s}{R_{b0}+R_{s0}}. \tag{14}$$

When eq. (14) is satisfied, the assumption is valid, and the volume flow between the big and small rings is non-existent. According to eq. (14), it follows that

$$V_{b0}=V_b,\ \ V_{s0}=V_s. \tag{15}$$

It can be concluded from eq. (15) that the volumes of the big and small rings of the blank must be equal to those of the rolled rings, respectively, to satisfy eq. (14). So, design method (A4) can be modified to be

$$\begin{aligned}&B_{b0}=B_b,\ B_{s0}=B_s,\ r_0=\frac{r}{K},\\ &R_{b0}=\sqrt{R_b^2+r_0^2-r^2},\ R_{s0}=\sqrt{R_s^2+r_0^2-r^2}.\end{aligned} \tag{16}$$

Under this design, the volume flow between the big and small rings is non-existent in rolling, and the blank can be formed as the specified rolled ring.

Taking ΔV_{b1}, ΔV_{b2} and ΔV_{b3} as the volume change amounts of the big ring under design methods (A1), (A2), (A3), respectively, and taking $\Delta V_b'=\Delta V_{b1}-\Delta V_{b2}$, $\Delta V_b''=\Delta V_{b2}-\Delta V_{b3}$, one obtains the expressions for $\Delta V_b'$ and $\Delta V_b''$ as follows, according to eqs. (11), (12) and (13).

$$\begin{aligned}\Delta V_b'&=\frac{\pi B_bB_sL_0(2R_{b0}-L_0)}{B},\\ \Delta V_b''&=\frac{\pi B_bB_s(L-L_0)(2R_{b0}-L_0-L)}{B}.\end{aligned} \tag{17}$$

According to geometrical relationships, $R_{b0}>L>L_0$. Then, $\Delta V_b'<0$ and $\Delta V_b''<0$.

As $\Delta V_{b1}>0$, $\Delta V_{b2}>0$ and $\Delta V_{b3}>0$, it follows that $\Delta V_{b1}>\Delta V_{b2}>\Delta V_{b3}$. So, it can be determined that the amount of volume flow from the small ring into the big ring under method (A1) is the greatest, and that under method (A3) is

the least.

3.2 Comparison among four design methods

To verify the theoretical analysis results and to determine the optimal blank design method, an example comparison among the four design methods was carried out based on FE simulation and rolling experiment. The dimensions of a stepped-section rolled ring are were given first, and the rolling ratio was 1.462. Then four blanks were designed, Blanks 1 to 4, corresponding to the design methods (A1) to (A4), respectively, as shown in Table 1. The dimensions of the rolls and the correlative technical parameters are shown in Table 2.

3.2.1 Simulative comparison

According to Tables 1 and 2, with the ABAQUS software, four 3-D FE models of stepped-section profile ring rolling were established. Because the four FE models have the same features, Figure 6 shows only the FE model for Blank 4.

The main features of the FE model are as follows.

1) The main roll takes active rotation. The mandrel takes linear feed motion and passive rotation. The guide roll takes translation motion, and its exterior surface keeps contact with the ring outer surface during the whole rolling process, to maintain the ring stability. Because the axial spread of the ring is negligible, the axial constraint is applied to the end surface of the blank, that is, axial displacement of the nodes on the ring end surface is not permitted.

2) Ring rolling simulation is considered as a quasi-static problem that does not consider inertial effect during the operation, thus the elastic-plastic explicit dynamic finite element method is used to avoid huge computation time and the convergence problem of the implicit procedure for the improvement of computational efficiency [12].

3) It is assumed that the frictions on the contact surfaces between the blank and the rolls meet the Coulomb friction law, both of the friction coefficients, between the main roll and the blank and between the mandrel and the blank, are taken as 0.15 [18], and the friction coefficient between the guide roll and the blank is taken as 0.

4) A uniform mesh with an 8-noded first-order reduction integration continuum element is adopted, and the ALE finite element formulation is used to control the mesh distortion [19].

The material of the blank is GCr15 bearing steel. Its density, Young's modulus and Poisson ratio are 7850 $kg \cdot m^{-3}$, 219.1 GPa and 0.3, respectively. And its elastic-plastic constitutive equation at room temperature is [20]

$$\begin{cases} \sigma = 219.1\varepsilon^e \text{ (GPa)}, & \varepsilon \leqslant 0.001856, \\ \sigma = [847(\varepsilon^p)^{0.129} + 30.37] \text{ (MPa)}, & \varepsilon > 0.001856, \end{cases}$$

where σ is the true stress, ε^e and ε^p are the true elastic strain and plastic strain, respectively, and ε is the true total strain.

Under the above conditions, the simulations of the four blanks were carried out. Figure 7 shows the cross-sections of the four blanks with different rolling times. It can be seen that the cross-sections of rolled Blanks 1, 2, 3 are not well-formed, due to volume flow from the small into the big ring and material accumulation, whereas the cross-section of rolled Blank 4 is well-formed because there is no volume flow or material accumulation. The volume flow amount from the small ring into the big ring under method (A1) is the greatest, and that under method (A3) is the least; it follows that the material accumulation of rolled Blank 1 is the greatest and that of rolled Blank 3 is the least.

In Figure 8, SDP represents the uniformity of the equi-

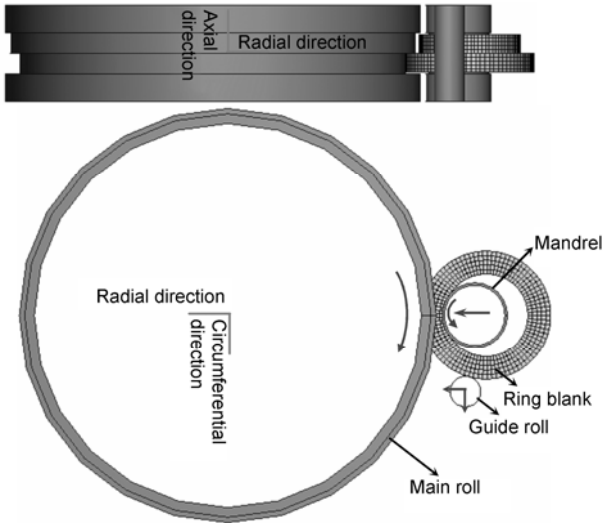

Figure 6 3-D FE model of stepped-section profile ring rolling.

Table 1 Dimensions of rolled ring and blanks

	Outer diameter of big ring D_b (mm)	Outer diameter of small ring D_s (mm)	Inner diameter d (mm)	Radial length of step L (mm)	Axial height of big ring B_b (mm)	Axial height of small ring B_s (mm)
Rolled ring	90	82	76	4	10	10
Blank 1	65.879	65.879	52	0	10	10
Blank 2	67.848	63.848	52	2	10	10
Blank 3	69.757	69.757	52	4	10	10
Blank 4	70.908	60.432	52	5.238	10	10

Table 2 Rolls dimensions and correlative technical parameters

Radius of outer surface of main roll		R_1	108 mm
Radius of large working surface of main roll		R_{1b}	106 mm
Radius of small working surface of main roll		R_{1s}	102 mm
Radius of outer surface of mandrel		R_2	13 mm
Radius of working surface of mandrel		R_{2w}	12 mm
Radius of working surface of guide roll		R_g	13 mm
Rotation speed of driving roll		n	2.43 r·s^{-1}
Feeding speed of mandrel		v	0.4 mm·s^{-1}
Rolling time	Blank 1	T	9.85 s
	Blank 2		7.31 s
	Blank 3		4.7 s
	Blank 4		6.14 s

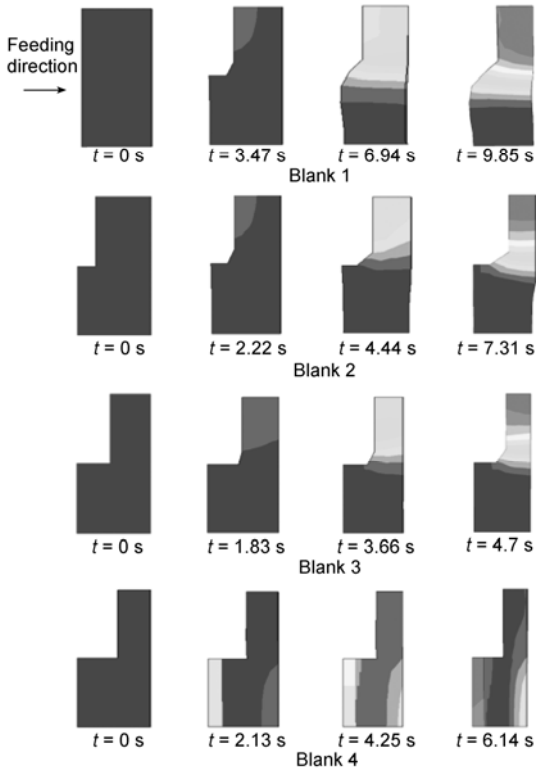

Figure 7 Cross-sections of four blanks with different rolling times.

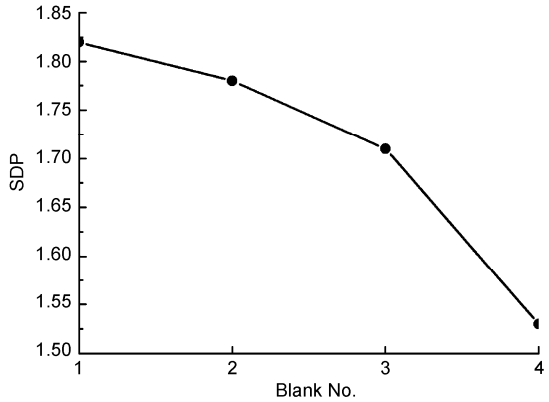

Figure 8 SDP values of four rolled blanks.

valent plastic strain distribution of the rolled blank, which is defined as [21]

$$\mathrm{SDP}=\sqrt{\sum_{i=1}^{N}((\mathrm{PEEQ}_i-\mathrm{PEEQ}_a)^2\cdot V_i)\Big/\sum_{i=1}^{N}V_i}\ , \qquad (18)$$

where $\mathrm{PEEQ}_a=\sum_{i=1}^{N}(\mathrm{PEEQ}_i\cdot V_i)/\sum_{i=1}^{N}V_i$. PEEQ_a is the average equivalent plastic strain (PEEQ), N is the number of elements of a ring, PEEQ_i is the PEEQ at element i, and V_i is the volume of element i.

The larger the SDP value, the more inhomogeneous the deformation of the blank, and the more likely the ring to produce inner flaws and surface cracks. As seen in Figure 8, the SDP value of the rolled blanks decreased from Blank 1 to Blank 4 because the material accumulation, caused by the volume flow, broke the original flow law of metal in rolling, and promoted the non-uniform metal flow and distribution. The larger the volume flow amount, the more severe the material accumulation, and the larger the SDP value.

3.2.2 Experimental comparison

Under simulation conditions, the rolls and the four blanks shown in Figure 9 were prepared, and the rolling experiments of the four blanks were performed on a D56G90 CNC cold ring rolling mill manufactured at KunShan, China, as shown in Figure 10.

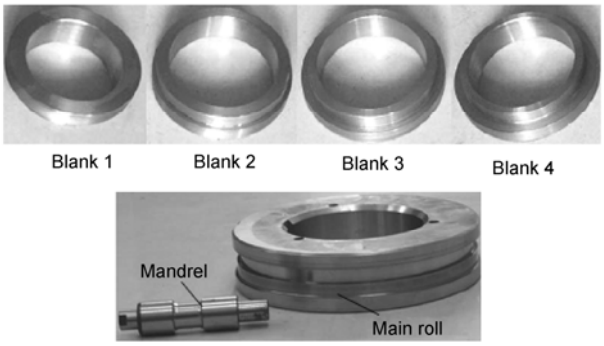

Figure 9 Rolls and four blanks.

Figure 10 D56G90 CNC cold ring rolling mill.

Figure 11 provides the final cross-sections of the four rolled blanks. It can be seen that material accumulation of varying degree was present at the step surfaces of rolled Blanks 1, 2, 3, and their cross-sections had bad shapes; whereas the step surface of rolled Blank 4 had no obvious material accumulation, and its cross-section had a good shape.

In Table 3, ε_b, ε_s and ε_d represent the dimension errors of the rolled blank, which are described as

$$\varepsilon_b = \frac{D_b - D_b'}{D_b} \times 100\%,$$
$$\varepsilon_s = \frac{D_s - D_s'}{D_s} \times 100\%, \quad (24)$$
$$\varepsilon_d = \frac{d - d'}{d} \times 100\%,$$

where D_b, D_s and d are the dimensions of the rolled ring. D_b', D_s' and d' are the dimensions of the rolled blank under the simulation and experiment.

Because material accumulation hinders the volume flow from the small ring into the big ring, the big and small rings deform deficiently. The greater the material accumulation, the less insufficiently the big and small rings deform. So, it can be seen from Table 3 that the dimension errors all decreased from rolled Blank 1 to rolled Blank 4.

The above comparison demonstrate that volume flow is disadvantageous for stepped-section profile ring rolling because it can result in material accumulation at the step surface of the rolled ring, which can hinder the step formation and ring enlargement. This result verifies the theoretical analysis of section 3.1. So, it can be concluded that the modified design method (A4) is the optimal blank design method for stepped-section profile ring rolling, because it does not lead to any volume flow between the rings.

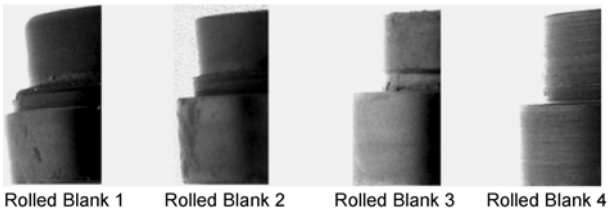

Figure 11 Final cross-sections of four rolled blanks.

The processing of stepped-section blanks is more complex than that of rectangular section blanks, thus the optimal blank design method may increase the difficulty of blank processing. Therefore, blank formability is usually regarded as the principal consideration in blank design. Although the rectangular section blank is easy to manufacture, its poor formability in stepped-section profile ring rolling may cause greater material consumption in the subsequent machining. The difference in material consumption between the stepped-section blank and the rectangular section blank is slight, because both are designed based on the volume conservation law. Furthermore, the current advanced blank processing techniques, like blocker-type forging and die forging, can easily process the stepped-section blank. So, it is believed that the optimal design method is feasible and can be realized in actual production.

4 Conclusions

This paper has proposed and evaluated four blank design methods for stepped-section profile ring rolling. The following conclusions can be drawn as follows.

1) Three of the four design methods can lead to material flow from the small ring into the big ring in the rolling process, while another design method does not.

2) Material flow, as described, is disadvantageous for the stepped-section profile ring rolling because it can lead to material accumulation at the step surface, which can hinder the step formation and ring enlargement.

3) Stepped-section blanks should be designed based on the principle that the volumes of the big and small blank rings are equal to those of the rolled ring, respectively. With this design method, a rolled ring with the best cross-sectional shape and the highest dimensional precision can be obtained.

However, the blank dimensions cannot be determined completely by the optimal design method, which also depend on the rolling ratio. Rolling ratio determines the blank dimensions and

Table 3 Dimensions of four rolled blanks under simulation and experiment

Rolled Blank		D_b' (mm)	D_s' (mm)	d' (mm)	ε_b %	ε_s %	ε_d %
Rolled Blank 1	Simulation	82.38	73.96	67.38	8.47	9.87	11.34
	Experiment	81.3	72.84	66.2	9.67	11.17	12.89
Rolled Blank 2	Simulation	85.4	77.12	70.8	5.11	5.95	6.84
	Experiment	84.38	76.06	69.68	6.24	7.2	8.32
Rolled Blank 3	Simulation	87.16	79.02	72.8	3.16	3.63	4.21
	Experiment	86.24	78.04	71.8	4.18	4.83	5.53
Rolled Blank 4	Simulation	89.66	81.64	75.62	0.38	0.44	0.5
	Experiment	89.1	81.06	74.98	1	1.15	1.34

reflects the deformation degree of the blank in rolling, thus it may influence the forming results such as force and power parameters, geometric accuracy and deformation non-homogeneity. So, a complete optimal blank design should also include how to determine the optimal value of the rolling ratio. A study of the effect of rolling ratio on stepped-section profile ring rolling is significant for blank design optimization, which will be carried out in our following work.

Supported by the Project of National Natural Science Foundation of China (Grant No. 50675164) and the Natural Science Foundation of China for Distinguished Young Scholars (Grant No. 50725517).

1 Eruc E, Shivpuri R. A summary of ring rolling technology-I. Recent trends in machines, processes and production lines. Int J Mach Tool Manu, 1992, 32(3): 379–398
2 Johnson W, MacLeod I, Needham G. An experimental investigation into the process of ring or metal type rolling. Int J Mech Sci, 1968, 10(6): 455–468
3 Mamalis A G, Johnson W, Hawkyard J B. On the pressure distribution between stock and rolls in ring rolling. J Mech Eng Sci, 1976, 18(4): 184–196
4 Hawkyard J B, Johnson W, Kirkland J. Analysis for roll force and torque in ring rolling with some supporting experiments. Int J Mech Sci, 1973, 15(11): 873–893
5 Mamalis A G, Johnson W, Hawkyard J B. Pressure distribution, roll force and torque in cold ring rolling. J Mech Eng Sci, 1976, 18 (4): 196–209
6 Lugora C F, Bramley A N. Analysis of spread in ring rolling. Int J Mech Sci, 1989, 29(2): 132–140
7 Yang D Y, Kim K H. Rigid plastic finite element analysis of plain strain ring rolling. Int J Mech Sci, 1988, 30(8): 571–580
8 Kim N, Machida S, Kobayashi S. Ring-rolling process simulation by three dimensional finite element method. Int J Mach Tool Manu, 1990, 30(4): 569–577
9 Xu S G, Lian J C, Howkyard J B. Simulation of ring rolling using a rigid plastic finite element model. Int J Mech Sci, 1991, 33(5): 393–401
10 Hua L, Zhao Z Z. The extremum parameters in ring rolling. J Mater Process Tech, 1997, 69(1-3): 273–276
11 Yan F L, Hua L, Wu Y Q. Planning feed speed in cold ring rolling. Int J Mach Tool Manu, 2007, 47(11): 1695–1701
12 Guo L G, Yang H, Zhan M. Research on plastic deformation behavior in cold ring rolling by FEM numerical simulation. Model Simul Mater Sci Eng, 2005, 13(7): 1029–1046
13 Qian D S, Hua L, Zuo Z J. Investigation of distribution of plastic zone in the process of plastic penetration. J Mater Process Tech, 2007, 187-188(1-3): 734–737
14 Yang H, Guo L G, Zhan M. Research on the influence of material properties on cold ring rolling processes by 3D-FE numerical simulation. J Mater Process Tech, 2006, 177(1-3): 634–638
15 Yang D Y, Kim K H, Hawkyard J B. Simulation of T-section profile ring rolling by the 3-D rigid-plastic finite element method. Int J Mech Sci, 1991, 33(7): 541–550
16 Li L Y, Yang H, Guo L G. Research on interactive influences of parameters on T-shaped cold ring rolling by 3D-FE numerical simulation. J Mech Sci Technol, 2007, 21(10): 1541–1547
17 Hua L, Huang X G, Zhu C D. Theory and Technology of Ring Rolling (in Chinese). Beijing: Mechanical Industry Press, 2001. 193–194
18 Hua L, Qian D S, Pan L B. Analysis of plastic penetration in process of groove ball-section ring rolling. J Mech Sci Technol. 2008, 22(7): 1374–1382
19 Davey K, Ward M J. A practical method for finite element ring rolling simulation using the ALE flow formulation. Int J Mech Sci, 2002, 44(1): 165–190
20 Qian D S, Hua L, Pan L B. Research on gripping conditions in profile ring rolling of raceway groove. J Mater Process Tech, 2009, 209(6): 2794–2802
21 Yang H, Wang M, Sun Z C. 3D coupled thermo-mechanical FE modeling of blank size effects on the uniformity of strain and temperature distributions during hot rolling of titanium alloy large rings. Comput Mater Sci, 2008, 44(2): 611–621